

**“ $J/\psi$ ’s Are Jazzy”**  
**G. E. Brown  $\sim$  1988**

R. Vogt

Lawrence Livermore National Laboratory, Livermore, CA 94551, USA  
Physics Department, University of California, Davis, CA 95616, USA

- Introduction
- How did I get into this?
- $J/\psi$ ’s are Hard :-(
  - Digging Deeper and More Broadly with the Hard Probes Cafe
    - Open Charm and  $J/\psi$  in  $pp$  Collisions
    - Cold Nuclear Matter Effects in  $pA$  and  $dA$  Collisions
- What’s New?

# Introduction to Quarkonium

$S$  state quarkonium detected through measurements of decays to lepton pairs,  $P$  states detected through radiative decays to an  $S$  state plus a photon

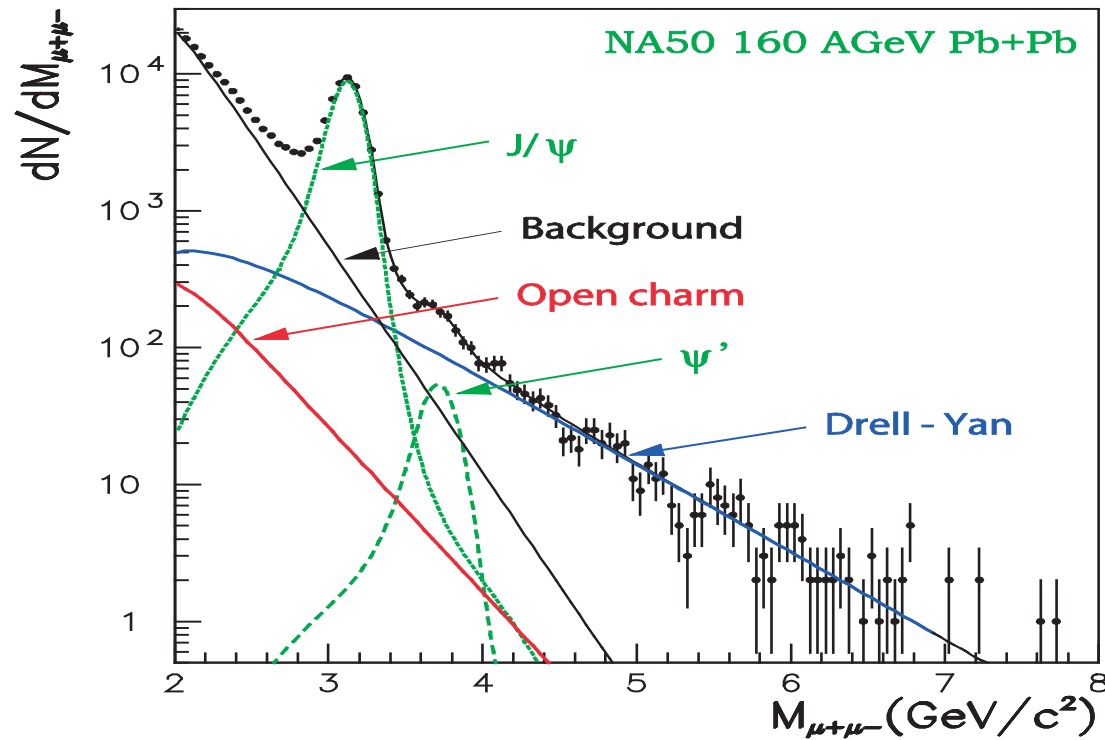


Figure 1: Example of contributions to the dimuon mass distribution at fixed-target energies.  $\Upsilon$  production is negligible at this energy.

# Charmonium States

State $\mathcal{C}$	$n^{2S+1}L_J$	$J^{PC}$	Mass (GeV)	$\text{B}(\mathcal{C} \rightarrow \mu^+\mu^-)$
$J/\psi$ [ $\psi(1S)$ ]	$1^3S_1$	$1^{--}$	<b>3.097</b>	$0.0588 \pm 0.0010$
$\chi_{c0}$	$1^3P_0$	$0^{++}$	<b>3.415</b>	—
$\chi_{c1}$	$1^3P_1$	$1^{++}$	<b>3.511</b>	—
$\chi_{c2}$	$1^3P_2$	$2^{++}$	<b>3.556</b>	—
$\psi'$ [ $\psi(2S)$ ]	$2^3S_1$	$1^{--}$	<b>3.686</b>	$0.0073 \pm 0.0008$

Table 1: Charmonium quantum numbers, spins and masses. The branching ratios to muon pairs are given for the quarkonium  $S$  states.

Separation of direct (and prompt) quarkonium production generally not straightforward due to feed down from higher states

Charmonium states further complicated by their non-prompt contributions from  $b$  meson decays,  $B \rightarrow J/\psi X$ ,  $\psi' X$ , and, at collider energies,  $W^- \rightarrow b\bar{c}X$  followed by  $b\bar{c} \rightarrow c\bar{c} \rightarrow J/\psi, \psi'$

# Charmonium Family

## Extracting direct production

- Subtract non-prompt decays ( $b$  quark sources)
- Remaining  $\psi'$  production is prompt
- Subtract  $\psi'$  contributions to inclusive  $J/\psi$
- Determine prompt  $\chi_{cJ}$  production from  $\chi_{cJ} \rightarrow J/\psi \gamma$  decays
- Subtract  $\chi_{cJ}$  contributions to inclusive  $J/\psi$
- Remaining  $J/\psi$  production is prompt

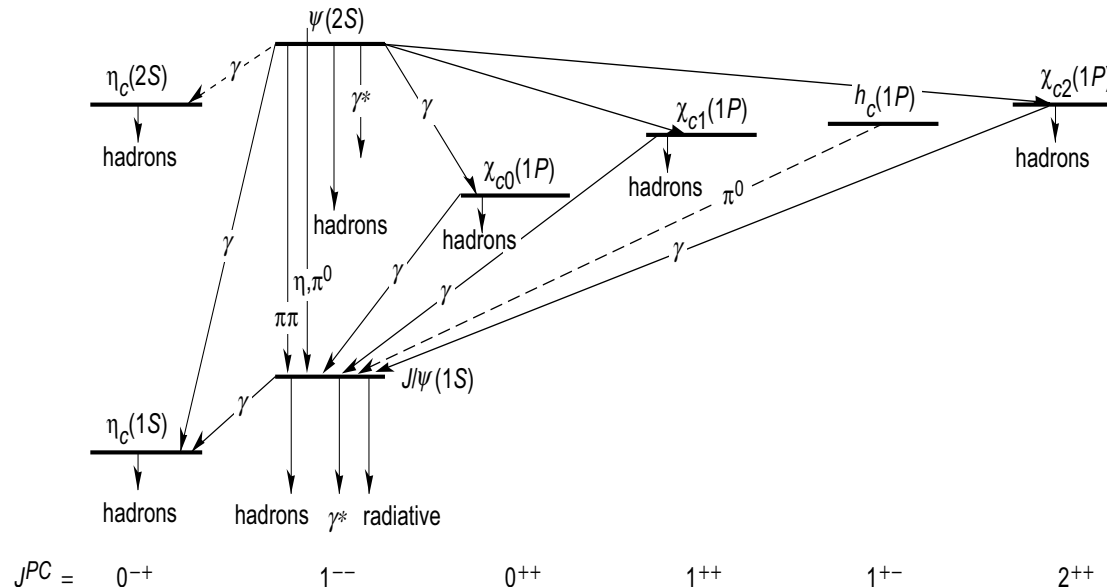


Figure 2: Spectrum of the charmonium family with important decay transitions between states highlighted.

How Did I Get Into This?

# My First Project

I joined the Stony Brook nuclear theory group right after my first year, working with Hans Hansson

My first paper though was with Andy Jackson the Younger on mass modifications of the charmonium states (potential model) and  $D$  mesons in medium (Bag model)

We showed that, with the temperature dependence assumed in the two approaches, one could perhaps see the  $\psi''$  in the dilepton decay channel (Ha! The  $\psi'$  is already hard enough): A. Jackson and R. V., Phys. Lett. B 206 (1988) 333

That project was the subject of my oral exam, on a Friday the 13th no less, with Gordon Baym in attendance (“Triskadecaphobes unite!” – Tom Ainsworth)

## Matsui and Satz

My first conference was at home, Gerry's birthday meeting in '86: "Windsurfing the Fermi Sea"

There I met someone else who's been a big influence in my life: Helmut Satz, who told me about a little paper he was finishing with Tetsuo Matsui ( $J/\psi$  Suppression by Quark Gluon Plasma Formation, Phys. Lett. B 178 (1986) 416 – 1823 citations)

The idea seemed too good to be true: in a quark-gluon plasma, the  $J/\psi$  breaks apart due to Debye screening and instead of a great big peak in the dilepton continuum, you have only the continuum left because 'the hadronic cross section for the  $J/\psi$  to interact with nucleons is negligible'

Well...

# A Dependence of Charmonium

OK, this data came later but there was already  $J/\psi$  photoproduction data from nuclear targets that showed, for  $\sigma_{pA} = \sigma_{pp}A^\alpha$ ,  $\alpha < 1$  – clearly the  $J/\psi$  interacts with *something*

Definite  $A$  dependence for quarkonium (N.B. E772 data showed little difference between *e.g.*  $J/\psi$  and  $\psi'$  while later experiments did)

Drell-Yan ( $q\bar{q} \rightarrow l^+l^-$ ) is effectively independent of  $A$

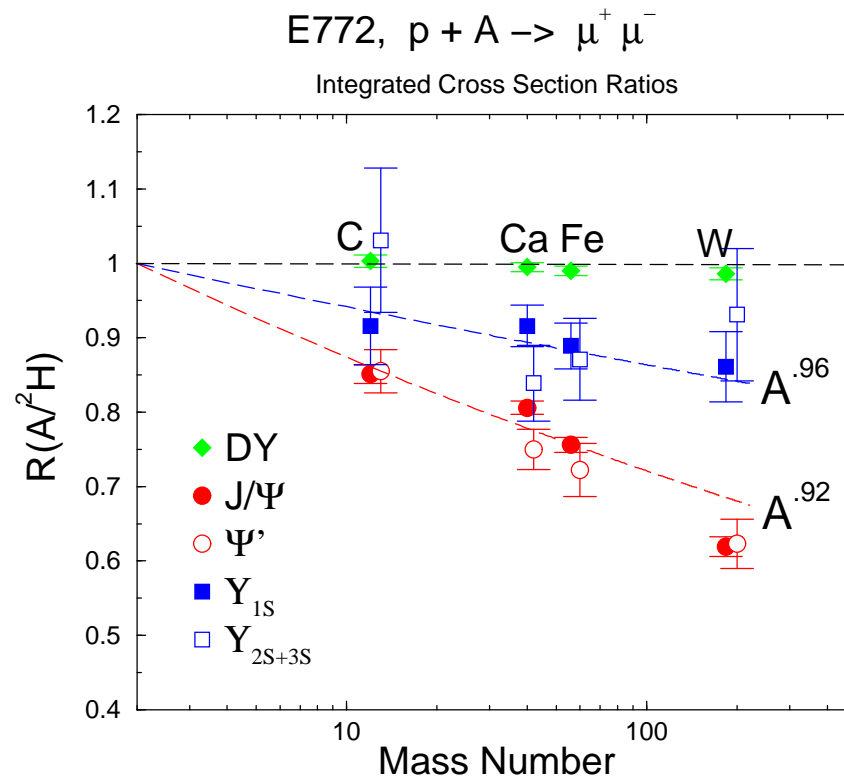


Figure 3: The  $A$  dependence of quarkonium and Drell-Yan production measured by E772.



## Then came the CERN SPS data

Clear suppression shown in O+U data, supplanted by S+U and Pb+Pb data but still suppression, just not total

Two different approaches taken to explain data without any plasma present: nuclear absorption (Gerschel & Hufner, others) and comovers (Gavin, Gyulassy, Jackson; Vogt, Prakash, Koch and Hansson, *etc*)

We had back to back articles in Phys. Lett. B 207 (1988): A Tale of Two Papers and there is not enough booze in the world to make me tell the full story here

Suffice it to say that it was at this point that Gerry told me “ $J/\psi$ ’s are jazzy” – too jazzy for a graduate student

Our paper was the first (I think) to consider hadronic interactions work both ways, we included a regeneration term that could lead to enhancement of the  $J/\psi$

Clearly Matsui & Satz was strawman to break down as too simplistic but alternative explanations not altogether easy

Still no completely satisfactory explanation for Pb+Pb (and In+In data, as Carlos Lourenco will gladly tell you) but no more SPS data so field has moved on

# SPS Data With Some Baseline

After many attempts to reanalyze, the SPS Pb+Pb data may or may not be ‘anomalous’ – they do require more than nuclear absorption (regeneration as well?) – but the S+U data are not

Things that have improved(?) since SPS: new ways to measure centrality and no further reliance on Drell-Yan as a baseline (now  $R_{AA}$ , a ratio relative to  $pp$ )

Things that have *not* improved: statistics – the fixed target program had millions of  $J/\psi$ ’s

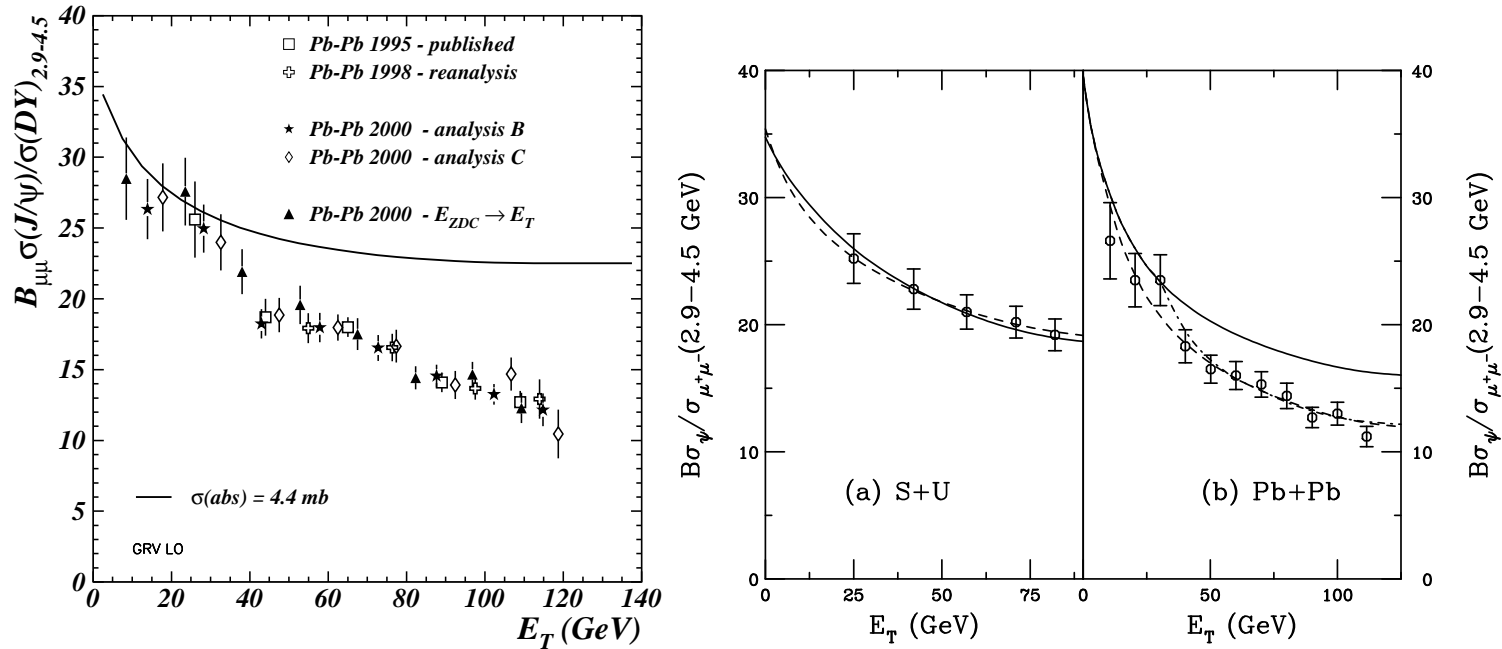


Figure 4: (Left) Compilation of Pb+Pb data taken by NA50. (Right) The calculated  $J/\psi$  to Drell-Yan ratios as a function of  $E_T$  are compared with data from (a) S+U (Phys. Lett. B 449 (1999) 128) and (b) Pb+Pb (Eur. Phys. J. C 39 (2005) 335) interactions. The solid curves show  $\sigma_{J/\psi N} = 4.8$  mb and  $\sigma_{J/\psi,dir}^{co} = 0.67$  mb. The dashed curve in (a) shows nuclear absorption alone with  $\sigma_{J/\psi N} = 7.3$  mb. Two additional calculations are shown in (b): increasing the participant density by a factor of two (dashed) and a quark-gluon plasma with  $n_f = 3$  (dot-dashed).

## $J/\psi$ 's Are *HARD*

We still can't even get  $pp$  production right

We don't have a clear handle on all aspects of  $J/\psi$  production in  $pA$

We're finally better able to describe hot matter effects (see review by Mocsy, Petreczky and Strickland (2013)) but the data continue to surprise, especially with excited states ( $\psi'$  for charmonium and  $\Upsilon(2S)$ ,  $\Upsilon(3S)$  for bottomonium)

# Digging Deeper and More Broadly with the Hard Probes Cafe

- Collaboration started by Helmut Satz in 1994
- Founding Members: H. Satz, X.-N. Wang, J. Cleymans, K. J. Eskola, R. V. Gavai, S. Gavin, S. Gupta, D. Kharzeev, E. Quack, K. Redlich, G. Schuler, K. Sridhar, D. K. Srivastava, P. V. Ruuskanen, R. L. Thews, and R. V.
- Meetings at CERN ('94), LBL ('94), ECT\* ('95), INT ('96), CFIF Lisbon ('97), INT ('98), JYFL Jyvaskyla ('99), BNL ('00), NBI ('01)
- Convener for open charm, quarkonium working group which has led to a long string of papers on higher order heavy flavor production in various systems
- Two volumes published: Int. J. Mod. Phys. A 10 (1995) and Int. J. Mod. Phys. E 12 (2003)
- Led directly to CERN Yellow Report in 2003
- So far six successful conferences in series 'Hard and Electromagnetic Probes of High-Energy Nuclear Collisions' (Hard Probes 2013 being the latest)

The rest of this talk is an update of where we are now on quarkonium (not that much better off really...  $J/\psi$ 's are still hard)

## Open Charm and $J/\psi$ in $pp$ Collisions

- Color Evaporation Model (CEM)
- Color Singlet Model (CSM)
- Nonrelativistic QCD (NRQCD) – also known as Color Octet Model (COM)
- Global Fits (CSM + COM)

# Color Evaporation Model

All quarkonium states are treated like  $Q\bar{Q}$  ( $Q = c, b$ ) below  $H\bar{H}$  ( $H = D, B$ ) threshold

Distributions for all quarkonium family members identical. Thus production ratios should also be independent of  $\sqrt{S}$ ,  $p_T$ ,  $x_F$ .

At LO,  $gg \rightarrow Q\bar{Q}$  and  $q\bar{q} \rightarrow Q\bar{Q}$ ; NLO add  $gq \rightarrow Q\bar{Q}q$

$$\sigma_Q^{\text{CEM}} = F_Q \sum_{i,j} \int_{4m_Q^2}^{4m_H^2} d\hat{s} \int dx_1 dx_2 f_{i/p}(x_1, \mu^2) f_{j/p}(x_2, \mu^2) \hat{\sigma}_{ij}(\hat{s}) \delta(\hat{s} - x_1 x_2 s)$$

First, values of  $m_Q$  and  $Q^2$  for several parton densities fixed from NLO calculation of  $Q\bar{Q}$  total cross sections

Inclusive  $F_Q$  fixed by comparison of NLO calculation of  $\sigma_Q^{\text{CEM}}$  to  $\sqrt{S}$  dependence of  $J/\psi$  and  $\Upsilon$  cross sections,  $\sigma(x_F > 0)$  and  $Bd\sigma/dy|_{y=0}$  for  $J/\psi$ ,  $Bd\sigma/dy|_{y=0}$  for  $\Upsilon$

Data and branching ratios used to separate the  $F_Q$ 's for each quarkonium state

Resonance	$J/\psi$	$\psi'$	$\chi_{c1}$	$\chi_{c2}$	$\Upsilon$	$\Upsilon'$	$\Upsilon''$	$\chi_b(1P)$	$\chi_b(2P)$
$\sigma_i^{\text{dir}}/\sigma_H$	<b>0.62</b>	<b>0.14</b>	<b>0.6</b>	<b>0.99</b>	<b>0.52</b>	<b>0.33</b>	<b>0.20</b>	<b>1.08</b>	<b>0.84</b>
$f_i$	<b>0.62</b>	<b>0.08</b>	<b>0.16</b>	<b>0.14</b>	<b>0.52</b>	<b>0.10</b>	<b>0.02</b>	<b>0.26</b>	<b>0.10</b>

Table 2: The ratios of the direct quarkonium production cross sections,  $\sigma_i^{\text{dir}}$ , to the inclusive  $J/\psi$  and  $\Upsilon$  cross sections, denoted  $\sigma_H$ , and the feed down contributions of all states to the  $J/\psi$  and  $\Upsilon$  cross sections,  $f_i$ , Digal *et al.*.

# $J/\psi$ Cross Sections from $c\bar{c}$ Fits

Take results of  $c\bar{c}$  fits, calculate NLO  $J/\psi$  cross section in CEM, fit scale factor  $F_C$  (needed to match the  $c\bar{c}$  cross section below the  $D\bar{D}$  threshold to the inclusive  $J/\psi$  cross section) with central value of parameter sets – tighter uncertainty band

CEM calculation reproduces shape of  $J/\psi$   $p_T$  and  $y$  distributions rather well with single parameter

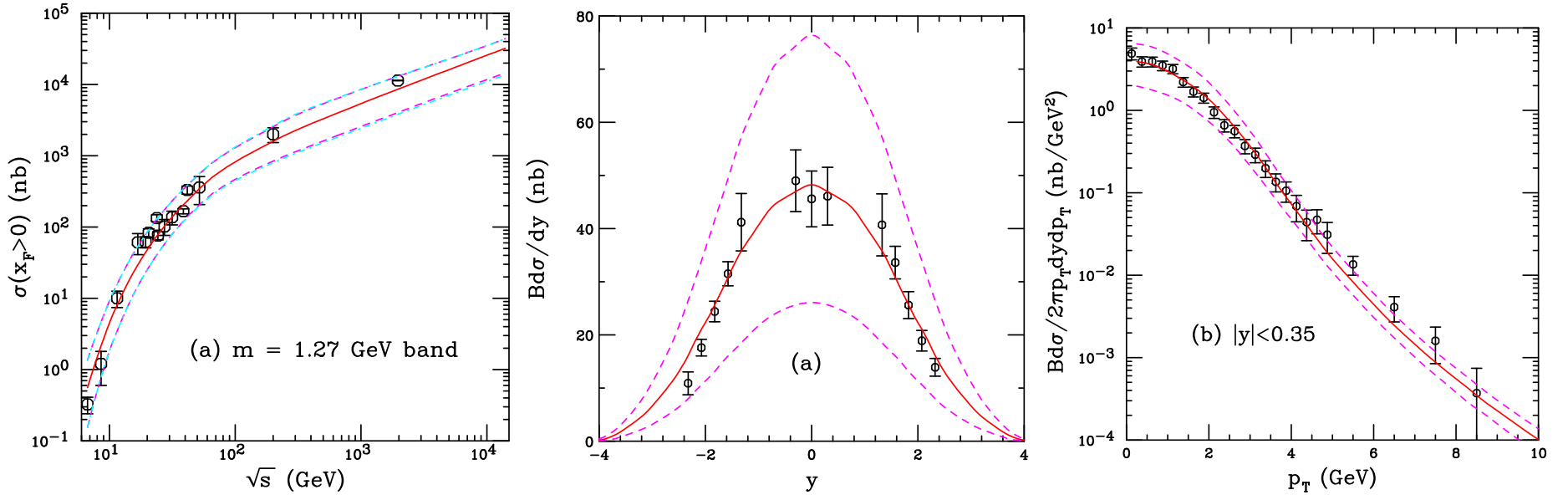


Figure 5: (Left) The uncertainty band on the forward  $J/\psi$  cross section. The dashed magenta curves and dot-dashed cyan curves show the extent of the corresponding uncertainty bands. The dashed curves outline the most extreme limits of the band. The  $J/\psi$  rapidity distribution (center) and the midrapidity  $p_T$  distributions (right) and their uncertainties. The results are compared to PHENIX  $pp$  measurements at  $\sqrt{s} = 200$  GeV. The solid red curve shows the central value while the dashed magenta curves outline the uncertainty band. A  $\langle k_T^2 \rangle$  kick of  $1.19 \text{ GeV}^2$  is applied to the  $p_T$  distributions. [R. Nelson, RV, and A.D. Frawley, PRC **87** (2013) 014908.]

# Color Singlet Model Production

CSM assumes factorization of production process into perturbative production of on-shell  $Q$  and  $\bar{Q}$  at scale  $m_T$  of the final state (assumes that the color and spin of the  $Q\bar{Q}$  pair is unchanged by binding)

The heavy quark velocity in the bound state must be small, thus it is assumed to be created with the heavy quarks at rest in the meson frame, the static approximation

Static approximation amounts to considering only first non-zero part of amplitude when the perturbative matrix element  $\mathcal{M}$  is expanded in powers of relative  $Q\bar{Q}$  momentum  $p$ ; for  $S$  states

$$\int dp \Phi(\vec{p}) \mathcal{M}(p) \delta(2p^0) \simeq \mathcal{M}(p=0) \Psi(\vec{x}=0)$$

Coordinate-space wavefunction  $\Psi$  is non-perturbative input which can be extracted from leptonic decay width:  $|\Psi(0)|^2$  for  $S$  states;  $|\Psi'(0)|^2$  for  $P$  states since  $|\Psi(0)| = 0$

At LO,  $S$  state production is by  $gg \rightarrow \psi g$  at  $\mathcal{O}(\alpha_s^3)$  while  $gg \rightarrow \chi_c$ ,  $\mathcal{O}(\alpha_s^2)$ , is allowed

Expectation that prompt  $J/\psi$  and  $\psi'$  production should be small and high  $p_T$   $J/\psi$ 's should come from  $\chi_c$  decays

**Strong disagreement with CDF production data, higher order CS contributions reduce disagreement with data but with growing uncertainty**



# Higher Order Corrections Improve CSM Agreement

Higher order contributions to the CSM: complete NLO and a partial NNLO (NNLO\*) results bring high  $p_T$  ( $p_T > 5$  GeV) quarkonium production into better agreement with Tevatron data at  $\sqrt{s} = 1.96$  TeV

$J/\psi$  and  $\psi'$  still below the data, cleaner  $\psi'$  has no feed down contribution (all prompt)

$\Upsilon(1S)$  calculation is prompt data (inclusive, *i.e.* with feed down included) times the direct fraction, essentially assuming that the feed down contribution has the same  $p_T$  distribution – similar to CEM

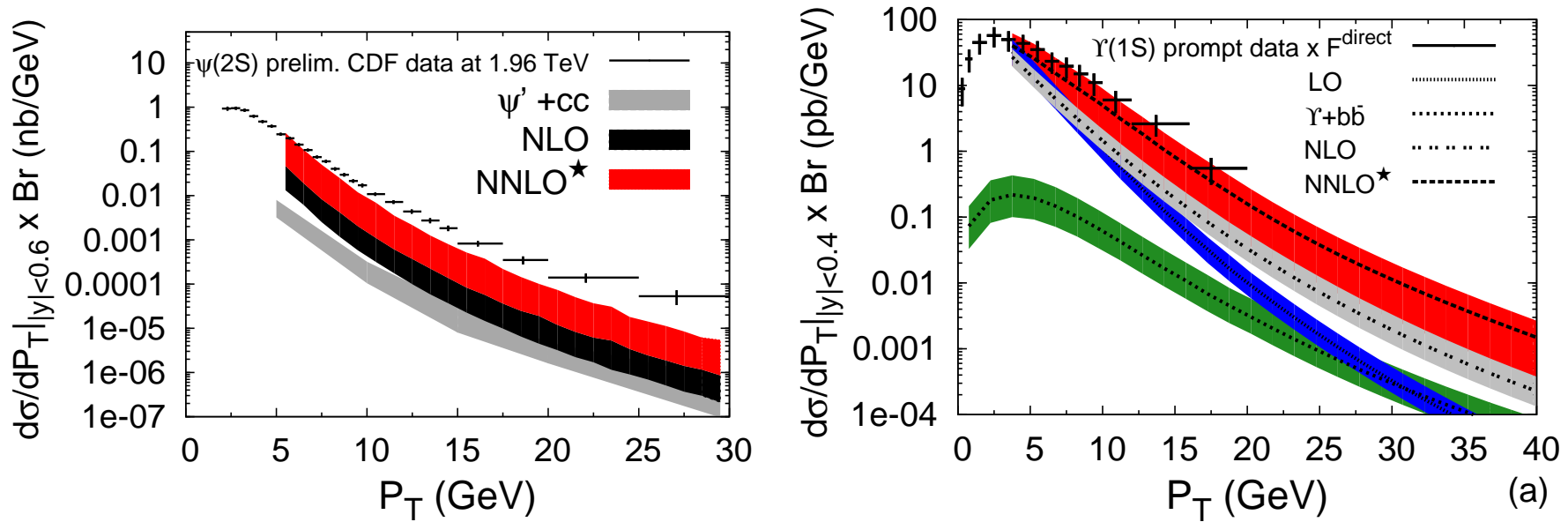


Figure 6: Recent CSM  $p_T$  distributions up to NLO and NNLO\* compared to (left)  $\psi'$  and (right)  $\Upsilon(1S)$  measurements by CDF at  $\sqrt{s} = 1.96$  TeV. [From QWG report, Eur. Phys. J C **71** (2011) 1534.]

# Color Octet (NRQCD) Production

New Fock states introduced to cancel infrared divergences in light hadron decays of  $\chi_{c1}$  into two gluons, one real and one virtual; when real gluon is soft, decay width diverges without new terms

These new Fock states included  $g c \bar{c} (^3S_1)$  color octet and introduced new momentum scale,  $\Lambda$ , for light quark

Based on systematic expansion in strong coupling constant,  $\alpha_s$ , and relative velocity of  $Q$  and  $\bar{Q}$ ,  $v$  (in bound states,  $v_c^2 \sim 0.23$  and  $v_b^2 \sim 0.08$ )

$$\begin{aligned} |\psi_c\rangle &= \mathcal{O}(1)|Q\bar{Q}[^3S_1^{(1)}]\rangle + \mathcal{O}(v)|Q\bar{Q}[^3P_J^{(8)}]_g\rangle + \mathcal{O}(v^2)|Q\bar{Q}[^3S_1^{(1,8)}]_{gg}\rangle + \mathcal{O}(v^2)|Q\bar{Q}[^1S_0^{(8)}]_g\rangle + \mathcal{O}(v^2)|Q\bar{Q}[^3D_J^{(1,8)}]_{gg}\rangle + \dots \\ |\chi_{cJ}\rangle &= \mathcal{O}(1)|Q\bar{Q}[^3P_J^{(1)}]\rangle + \mathcal{O}(v)|Q\bar{Q}[^3S_1^{(8)}]_g\rangle \end{aligned}$$

Factorization between short distance, perturbative, contribution and non-perturbative hadronization, described by non-perturbative matrix elements in limit of large heavy quark mass

NRQCD includes color singlet and color octet matrix elements

- Two different color singlet matrix elements in NRQCD, one for production and one for decay – can be different even though  $\langle \mathcal{O}^3S_1[^3S_1^{(1)}] \rangle \propto |\Psi(0)|^2$  up to order  $v^4$
- Perturbative octet amplitudes for  $^1S_0^{(8)}$  and  $^3P_0^{(8)}$  have the same  $p_T$  dependence so they can't be separated, thus a linear combination  $\langle \mathcal{O}[^1S_0^{(8)}] \rangle + k \langle \mathcal{O}[^3P_0^{(8)}] \rangle / m_Q^2$  where  $k$  is the ratio of the two amplitudes, typically different for high  $p_T$  and fixed-target energies

# Combined Color Singlet/Color Octet Global Fit

Global analysis of Butenschon and Kniehl attempts to make global fit to inclusive  $J/\psi$  data from RHIC, Tevatron, LHC (all hadroproduction), and HERA (electroproduction)

Fit LO and NLO color singlet (CS) and NRQCD (CS + CO) calculations to data  
Instead of fitting octet matrix elements to individual data sets, they attempt to obtain universal matrix elements

- Assume a given value of charm quark mass and scales for calculation
- Fit matrix elements with those parameters
- Determine uncertainties on fit results by keeping matrix elements and quark mass fixed, varying scale parameters by a factor of two around central value

Some caveats:

- Analysis limited to high  $p_T$  prompt  $J/\psi$  only
- Feed down either neglected or subtracted, assumes that the shape of the  $\chi_c$  and  $\psi'$  distributions same as  $J/\psi$
- No comparison to fixed-target total cross sections
- No attempt to determine how matrix elements depend on quark mass or scale

# Global Analysis: PHENIX at RHIC and CDF at the Tevatron

Only NLO CS+CO contributions realize agreement with data

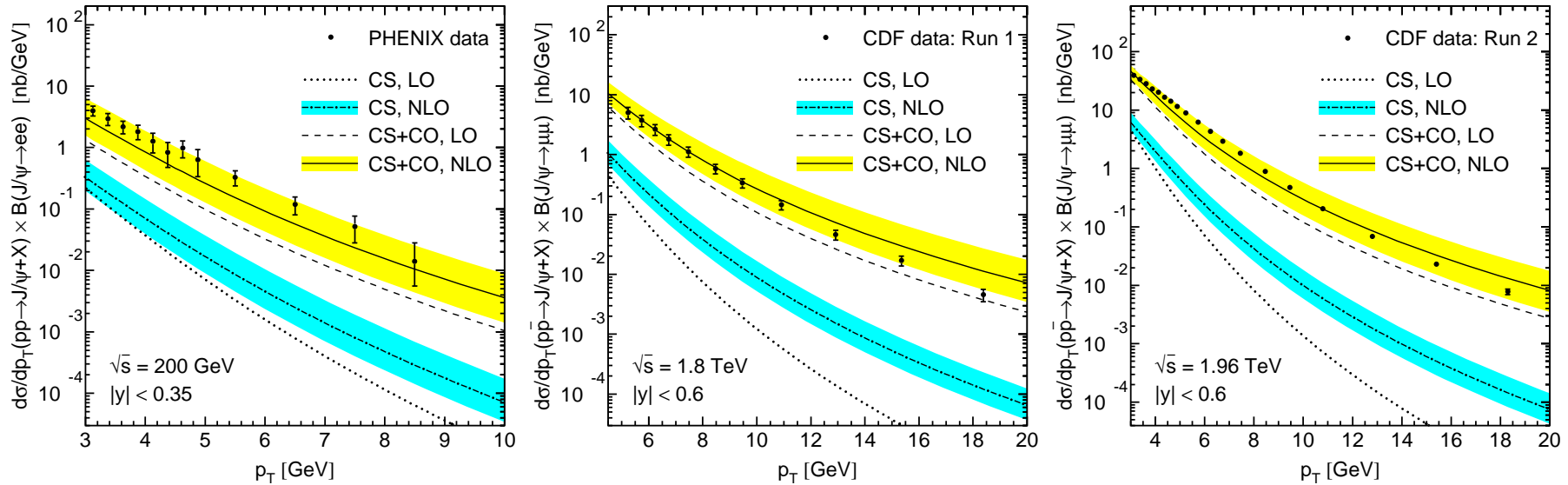


Figure 7: NLO NRQCD fit compared to the PHENIX (RHIC,  $\sqrt{s} = 200$  GeV) and CDF (Tevatron,  $\sqrt{s} = 1.96$  TeV) data. [Butenschon and Kniehl PRD **84** (2011) 051501]

# Polarization Crucial Test of Production Models

At large  $p_T$ , the dominant mechanism of quarkonium production is gluon fragmentation into a color octet  $Q\bar{Q}$  ( $c\bar{c}[^3S_1^{(8)}]$ )

Fragmenting gluon is nearly on mass shell and thus transversely polarized, polarization should be retained during hadronization

Polarized cross section,  $W \approx 1 + \lambda_\theta \cos^2 \theta$  with  $\lambda_\theta = 1$ , transverse polarization; 0, no polarization;  $-1$ , longitudinal polarization

Results shown in helicity frame, LO CSM and NRQCD calculations give transverse polarization, NLO CSM gives longitudinal polarization

Neither gives good description of Tevatron and ALICE data so far

Dependence on  $p_T$  cut? (Carlos Lourenco, HP2013, Stellenbosch)

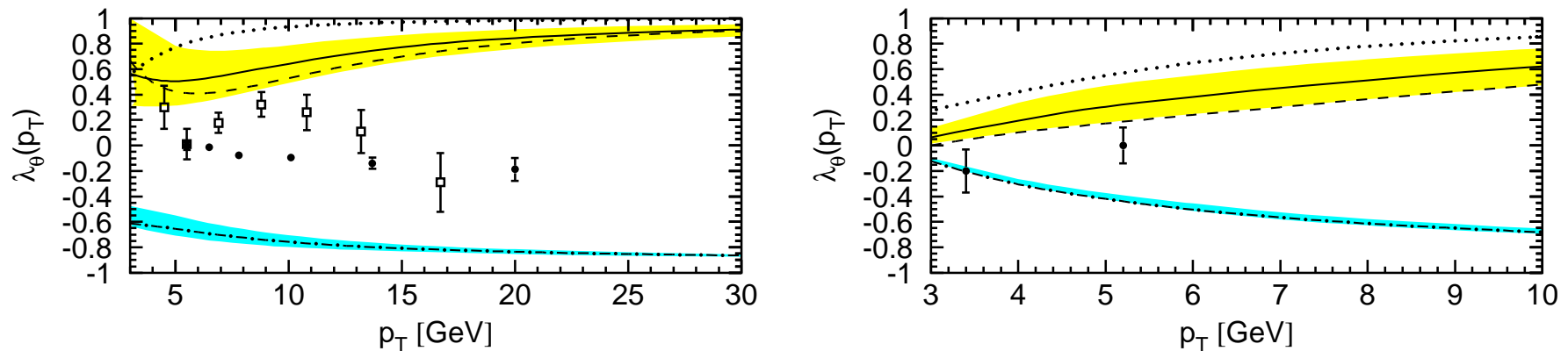


Figure 8: The  $J/\psi$  polarization at the Tevatron (left) and at ALICE (right) compared to LO CSM (dotted); NLO CSM (cyan dot-dashed), LO NRQCD (dashed), NLO NRQCD (yellow solid). [Butenschon and Kniehl, PRL **108** (2012) 172002]

# Cold Nuclear Matter Effects in $pA$ and $dA$ Collisions

# Cold Nuclear Matter Effects

Important cold nuclear matter effects include:

- Final-state absorption on nucleons — after  $c\bar{c}$  that forms the  $J/\psi$  has been produced, pair breaks up in matter due to interactions with nucleons
- Initial-state nuclear effects on the parton densities (shadowing) — affects total rate, important as a function of  $y/x_F$
- Energy loss — *either* initial-state effect, elastic scatterings of projectile parton before hard scattering creating quarkonium state, need to study Drell-Yan production to get a handle on the strength when shadowing is included — *or* final-state effect, scattering of the  $c\bar{c}$  or  $J/\psi$  after production — can be related to  $p_T$  broadening
- Intrinsic heavy flavors (Brodsky *et al*)

Shadowing strongly rapidity dependent

Absorption is rapidity and energy dependent (should vanish at high  $\sqrt{s}$ )

Energy loss and intrinsic heavy flavor more important at forward rapidity

# Cold Matter Effects on Heavy Flavor Production

Production cross section in a  $pA$  collision

$$\sigma_{pA}(S, m^2) = \sum_{i,j=q,\bar{q},g} \int_{4m_Q^2/S}^1 \frac{d\tau}{\tau} \int d^2b dz d\epsilon dx_1 dx_2 \delta(x_1 x_2 - \tau) \delta(x'_F - x_F - \delta x_F(\epsilon)) \delta(x'_F - x_1 + x_2) \\ \times P(\epsilon) S_A^{\text{abs}}(\vec{r}, z) f_i^p(x_1, \mu_F^2) F_i^A(x'_1, \mu_F^2, \vec{b}, z) \widehat{\sigma}_{ij}(s, m^2, \mu_F^2, \mu_R^2)$$

Survival probability for absorption of a (proto)charmonium state in nuclear matter

$$S_A^{\text{abs}}(b, z) = \exp \left\{ - \int_z^\infty dz' \rho_A(b, z') \sigma_{\text{abs}}(z - z') \right\}$$

$P(\epsilon)$  is energy loss probability that modifies the  $x_F$  of the produced  $J/\psi$  state

Nuclear parton densities

$$F_i^A(x, Q^2, \vec{b}, z) = \rho_A(s) S^i(A, x, Q^2, \vec{b}, z) f_i^p(x, Q^2) ; \quad s = \sqrt{b^2 + z^2} ; \quad \rho_A(s) = \rho_0 \frac{1 + \omega(s/R_A)^2}{1 + \exp[(s - R_A)/d]}$$

$S^i$  is shadowing parameterization for parton  $i$ , *e.g.* EPS09, EKS98, nDSg, DSSZ

With no nuclear modifications,  $S^i(A, x, Q^2, \vec{r}, z) \equiv 1$

Initial assumption that shadowing strength proportional to nuclear thickness raised to a power  $n$ , with appropriate normalization factor

EPS09s parameterization keeps powers  $n = 1 \cdots 4$  for  $A$ -independent coefficients

$$M_{\text{shad}} = 1 - (1 - S^g(x, Q^2)) \left( \frac{T_A^n(b)}{a(n)} \right)$$

If onset of shadowing is like a step function with a radius  $R$  and diffuseness  $d$

$$M_{\text{shad}} = 1 - \left( \frac{1 - S^g(x, Q^2)}{a(R, d)(1 + \exp((b - R)/d))} \right)$$



## $J/\psi$ $A$ Dependence vs. $x_2$ and $y_{\text{cm}}$

Effective  $\alpha$  ( $\sigma_{pA}/\sigma_{pp} = A^\alpha$ ) dissimilar as a function of  $x_2$ , closer to scaling for  $y_{\text{cm}}$  ( $x_1$ ) – higher  $\sqrt{s}$  stretches  $x$  values relative to rapidity ( $x_F = (2m_T/\sqrt{s}) \sinh y = x_1 - x_2$ )

Translating  $A$  dependence into effective absorption cross section,  $\sigma_{\text{abs}}$ , including shadowing effects, shows the  $x_F$  dependence of remaining cold matter effects

At negative  $x_F$ , HERA-B result suggests a negligible effective  $\sigma_{\text{abs}}$

Argument for more physics at forward  $x_F$  than accounted for by nuclear shadowing: energy loss?

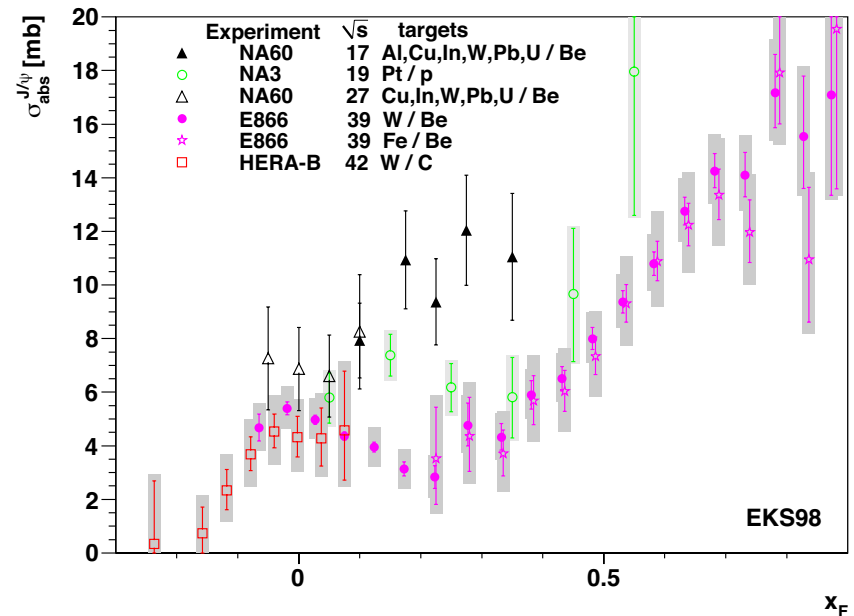
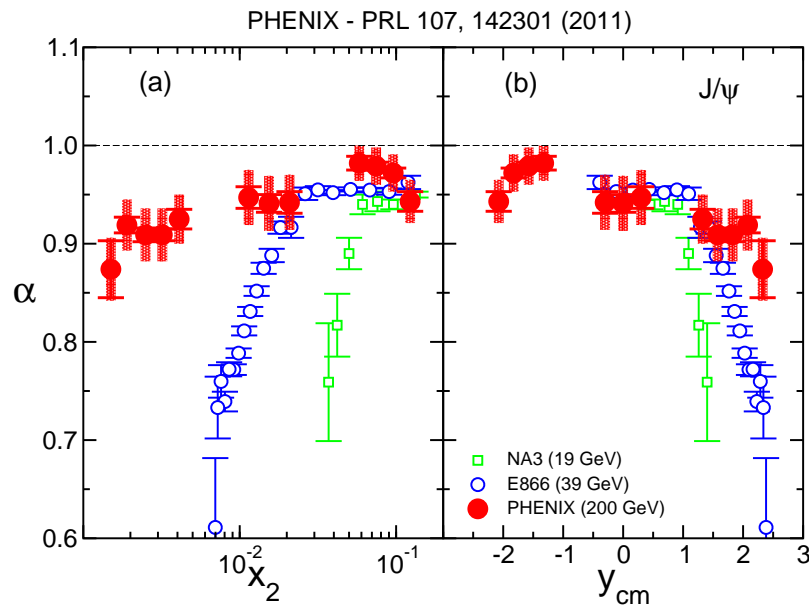


Figure 9: (Left) Comparison of effective  $\alpha$  for NA3, E866 and PHENIX. (Mike Leitch) (Right) Comparison of effective  $\sigma_{\text{abs}}$  for  $J/\psi$  (from QWG report, 2010).

# Shadowing

# Parton Densities Modified in Nuclei

Nuclear deep-inelastic scattering measures quark modifications directly; Drell-Yan and  $\pi^0$  measurements provide further information

More uncertainty in nuclear gluon distribution, only indirectly constrained by  $Q^2$  evolution, large uncertainties still remain, including LO vs NLO

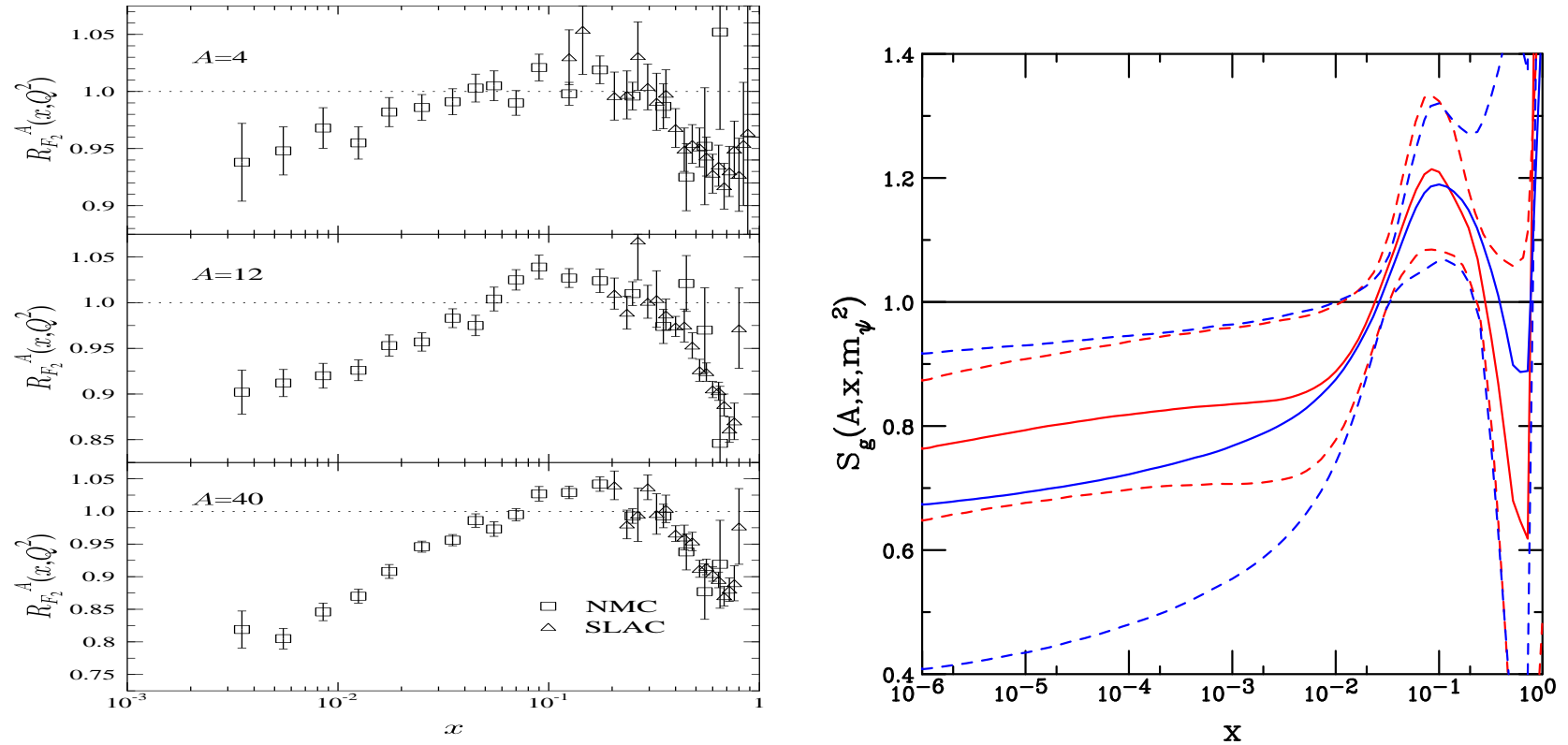


Figure 10: (Left) Ratios of charged parton densities in He, C, and Ca to D as a function of  $x$ . [From K.J. Eskola.] (Right) The modification of the gluon densities at LO (blue) and NLO (red) with EPS09, including uncertainties (dashed lines), calculated at  $m_\psi$ . (RV)

# Stronger Than Linear Impact Parameter Dependence?

RHIC minimum bias (impact-parameter integrated shadowing) d+Au data agrees with EPS09 shadowing and  $\sigma_{\text{abs}} = 4$  mb

The  $R_{CP}$  ratio does not agree with the impact-parameter dependent shadowing calculation (assuming dependence on  $T_A(b)$ ) at forward rapidity because the peripheral result is overestimated

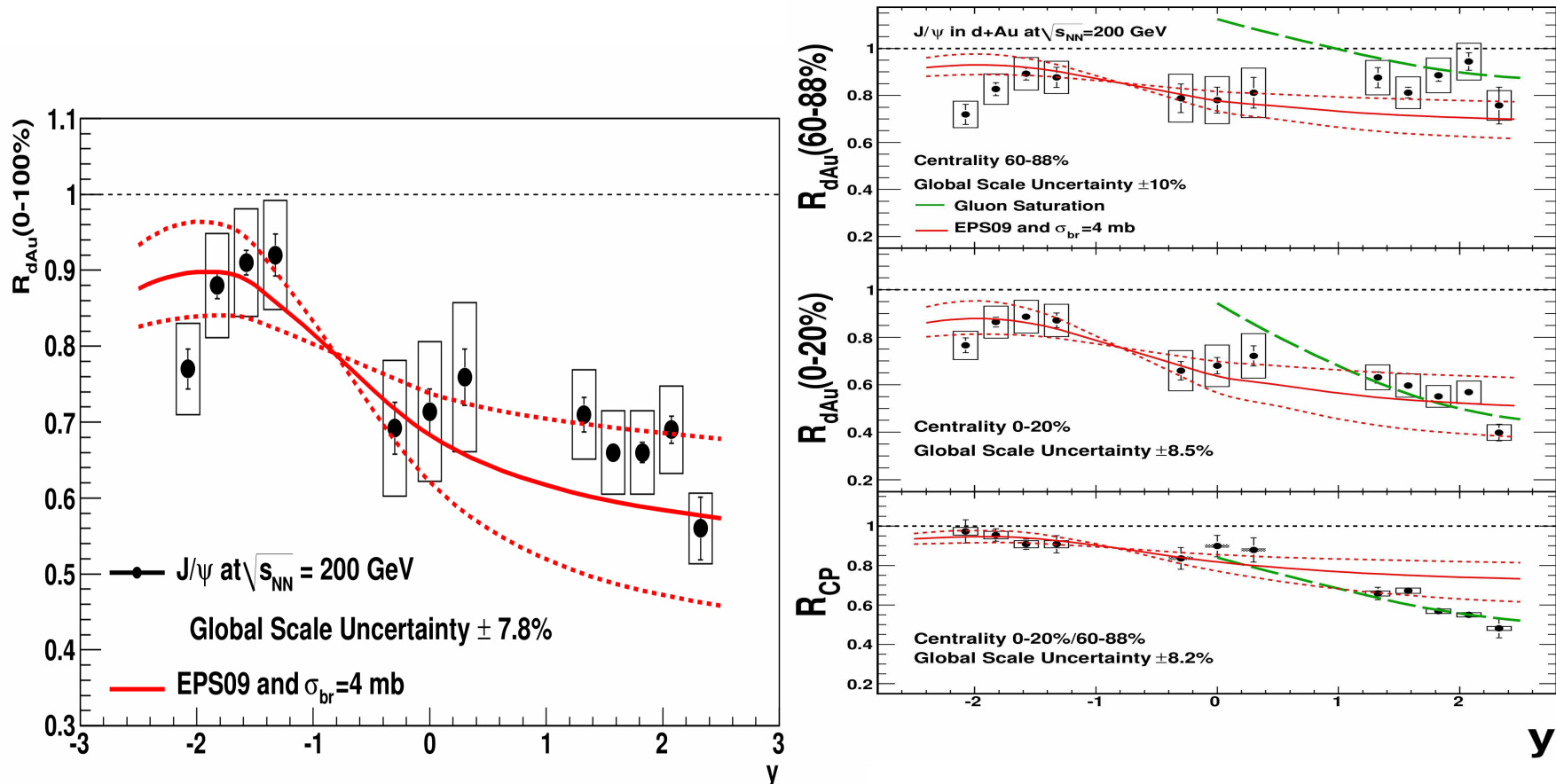


Figure 11: The PHENIX data compared to calculations of EPS09 shadowing including uncertainties and a constant absorption cross section of 4 mb. Left: the minimum bias result. Right: Including impact-parameter dependent shadowing in the 60 – 88% centrality (top) and 0 – 20% centrality (middle) bins. The lower panel shows the central-to-peripheral ratio. The dashed curves show a gluon saturation calculation.

# Impact Parameter Dependence of Shadowing on $J/\psi$ ?

Onset of shadowing with impact parameter  $r_T$  consistent with shadowing effects concentrated in core of nucleus where nucleons are more densely packed

Sharp onset of shadowing gives smaller effective absorption cross sections than linear dependence but does not change overall shape

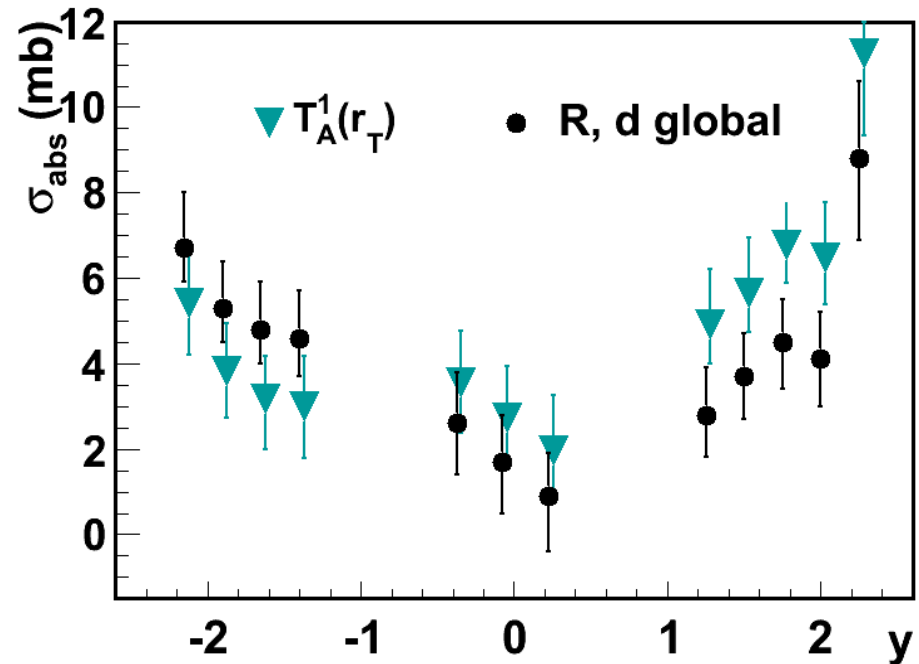
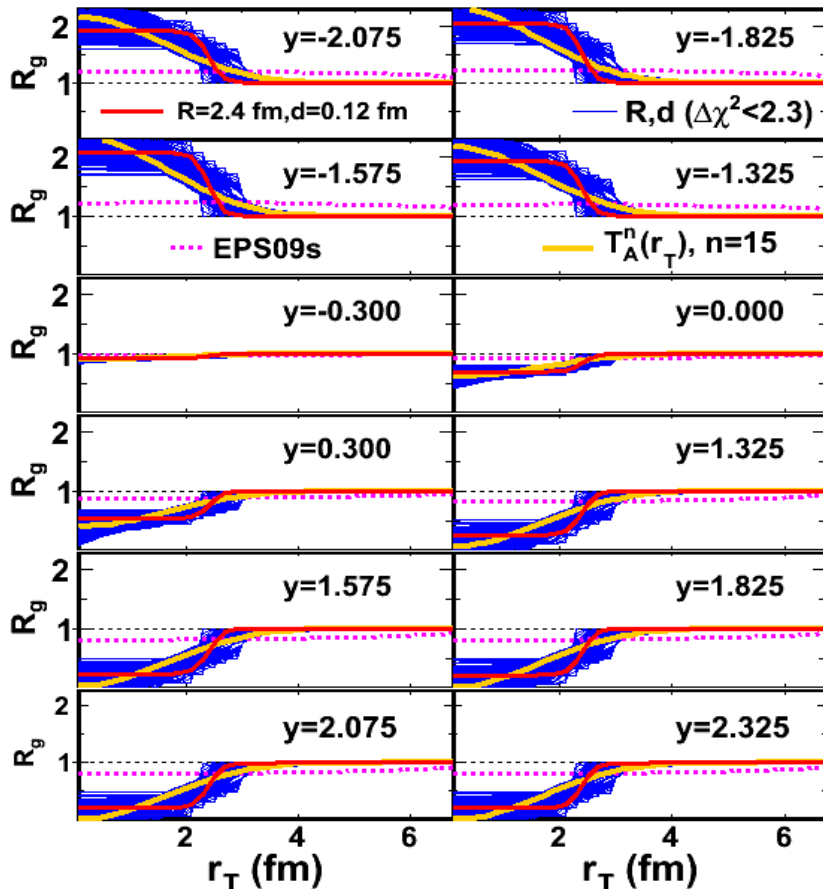


Figure 12: (Left) The gluon modification from the best fit global  $R$  and  $d$  (solid red line), along with results for all combinations of  $R$  and  $d$  within the  $\Delta\chi^2 = 2.3$  fit contour (thin blue lines). The modification from  $T_A^n(r_T)$  ( $n = 15$ ) is shown by the solid orange line. The dashed magenta line is the EPS09s impact parameter dependence. (Right) Comparison of  $\sigma_{\text{abs}}$  extracted from the PHENIX data assuming a linear dependence on nuclear thickness with those extracted using global values of  $R$  and  $d$ . [D. McGlinchey, A. D. Frawley and RV, Phys. Rev. C **87** (2013) 054910.]

# Nuclear Absorption

# Energy Dependence of $\sigma_{\text{abs}}^{J/\psi}$

At midrapidity, there seems to be a systematic decrease of the absorption cross section with energy independent of shadowing, trend continues at RHIC

$\sigma_{\text{abs}}^{J/\psi}(y_{\text{cms}} = 0)$  extrapolated to 158 GeV is significantly larger than measured at 450 GeV, underestimating “normal nuclear absorption” in SPS heavy-ion data

Calculations confirmed by NA60  $pA$  measurements at 158 GeV (QM09)

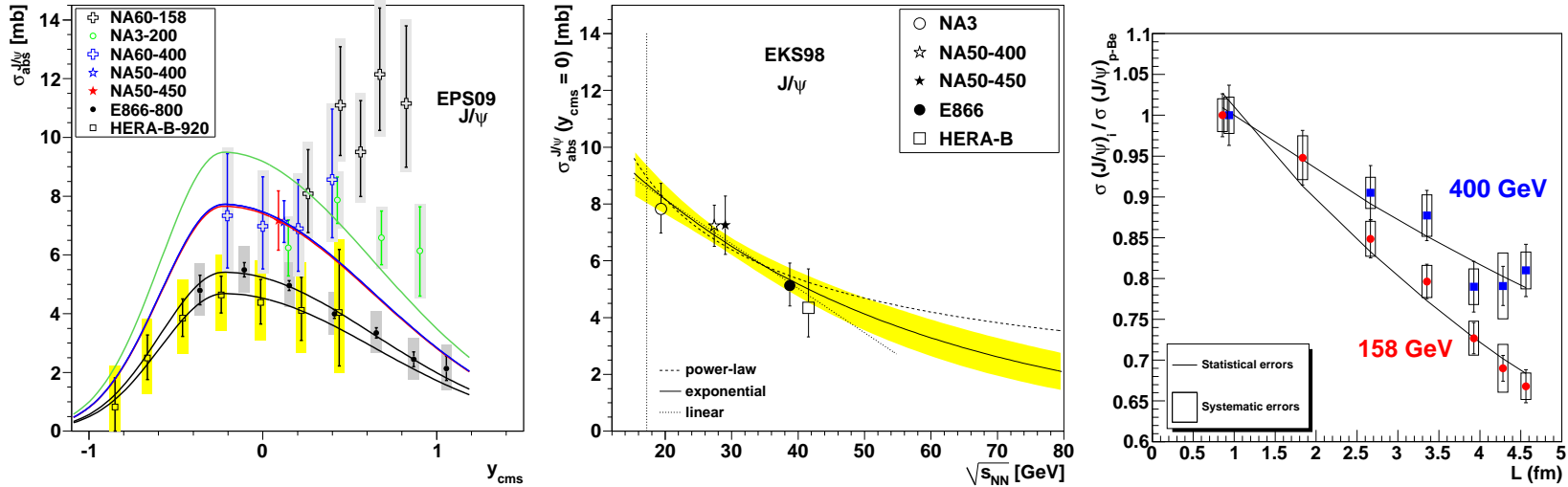


Figure 13: Left: Dependence of  $\sigma_{\text{abs}}^{J/\psi}$  on  $y_{\text{cms}}$  for all available data sets including EPS09 shadowing. The shape of the curves is fixed by the E866 and HERA-B data. [Loureño, RV, Wöhri] Middle: The extracted energy dependence of  $\sigma_{\text{abs}}^{J/\psi}$  at midrapidity for power law (dashed), exponential (solid) and linear (dotted) approximations to  $\sigma_{\text{abs}}^{J/\psi}(y = 0, \sqrt{s_{NN}})$  using the EKS98 shadowing parameterization with the CTEQ61L parton densities. The band around the exponential curve indicates the uncertainty in the extracted cross sections at  $x_F \sim 0$  from NA3, NA50 at 400 and 450 GeV, E866 and HERA-B. The vertical dotted line indicates the energy of the Pb+Pb and In+In collisions at the CERN SPS. [Loureño, RV, Wöhri] Right: The  $J/\psi$  cross section ratios for  $pA$  collisions at 158 GeV (circles) and 400 GeV (squares), as a function of  $L$ , the mean thickness of nuclear matter traversed by the  $J/\psi$ . [Arnaldi, Cortese, Scomparin]

## $\sigma_{\text{abs}}$ Grows with time $c\bar{c}$ Spends Traversing Nucleus

Mid- and backward rapidity  $J/\psi$  at  $\sqrt{s_{NN}} = 200$  GeV (longer  $\tau = L/\gamma$ ) dominated by conversion of color octet  $c\bar{c}$  pair to color singlet  $J/\psi$  by gluon emission

$$\sigma_{\text{abs}}(\tau) = \sigma_1 \left( \frac{\sqrt{s}}{10 \text{ GeV}} \right)^{0.4} \left( \frac{r_{c\bar{c}}(\tau)}{r_{J/\psi}} \right)^2 \quad r_{c\bar{c}}(\tau) = r_0 + v_{c\bar{c}}\tau \text{ for } r_{c\bar{c}}(\tau) < r_\psi$$

Different physics at forward rapidity where conversion takes place outside target

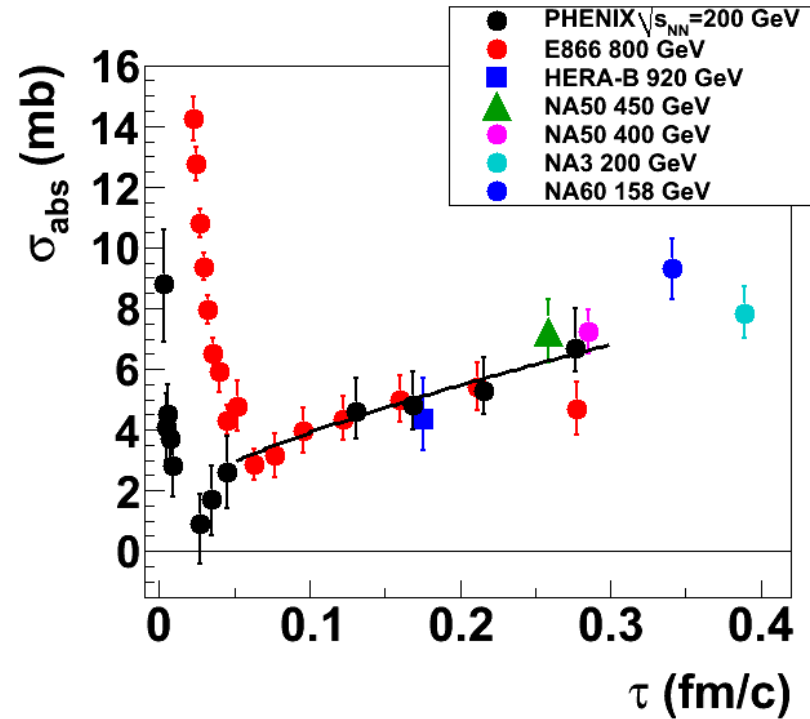


Figure 14: The effective  $c\bar{c}$  breakup cross section as a function of the proper time spent in the nucleus,  $\tau$ . The values were extracted from PHENIX  $\sqrt{s_{NN}} = 200$  GeV d+Au data after correction for shadowing using EPS09 and from fixed-target p+A data measured by E866 at 800 GeV, by HERA-B at 920 GeV, by NA50 at 450 GeV and 400 GeV, by NA3 at 200 GeV, and by NA60 at 158 GeV. In all fixed-target cases, the EKS98 parameterization was used. The curve is calculated based on octet-to-singlet conversion inside the nucleus. [D. McGlinchey, A. D. Frawley and RV, Phys. Rev. C **87** (2013) 054910.]



# A Dependence of $J/\psi$ and $\psi'$ Not Identical: Size Matters

Color octet mechanism suggested that  $J/\psi$  and  $\psi'$   $A$  dependence should be identical — Supported by large uncertainties of early data

More extensive data sets (NA50 at SPS, E866 at FNAL) show clear difference at midrapidity [NA50  $\rho L$  fit gives  $\Delta\sigma = \sigma_{\text{abs}}^{\psi'} - \sigma_{\text{abs}}^{J/\psi} = 4.2 \pm 1.0$  mb at 400 GeV,  $2.8 \pm 0.5$  mb at 450 GeV for absolute cross sections]

Suggests we need to include formation time effects

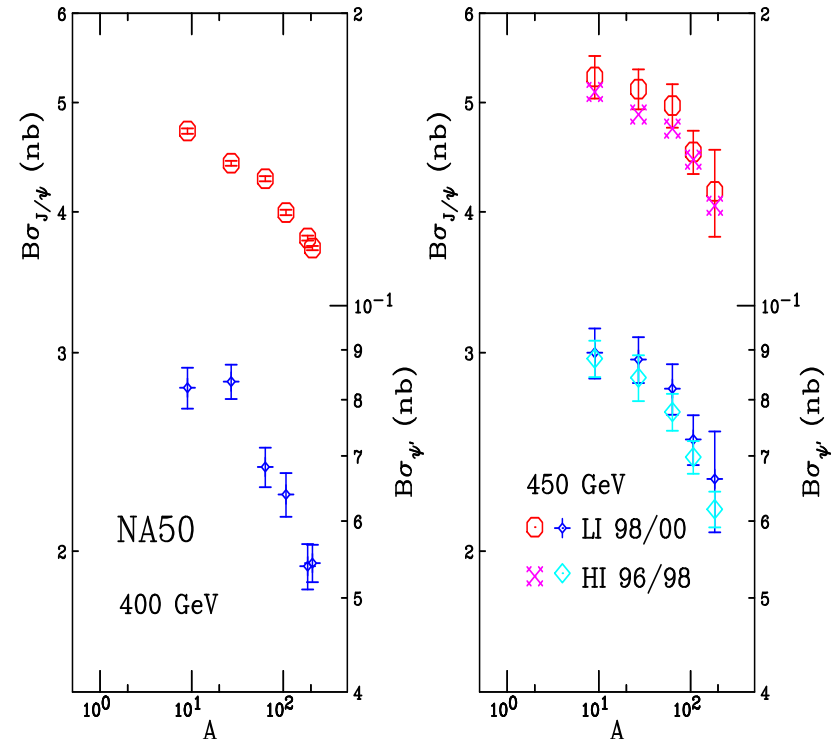
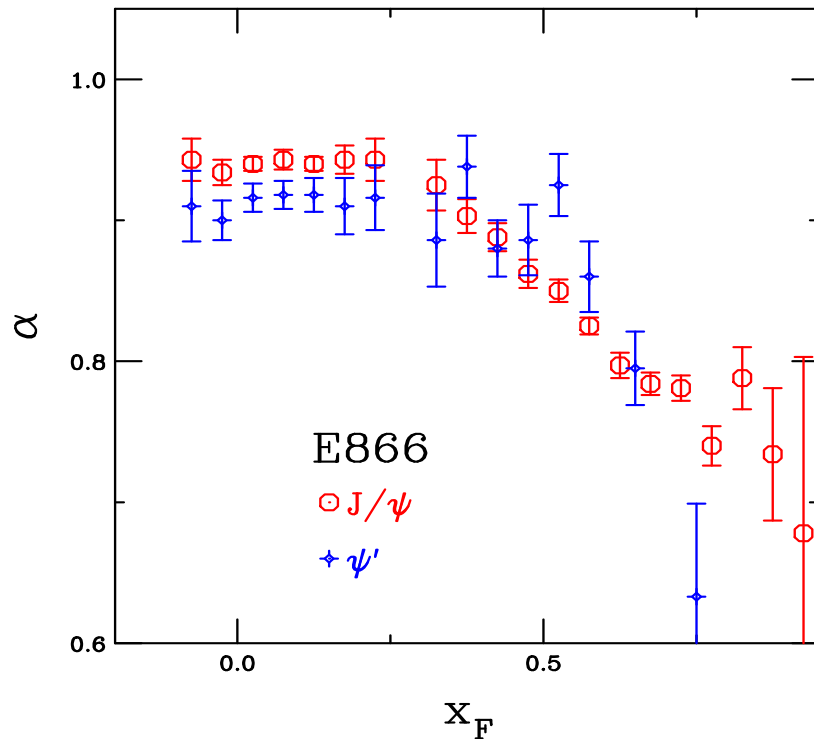


Figure 15: The  $J/\psi$   $A$  dependence (left) as a function of  $x_F$  at FNAL ( $\sqrt{s_{NN}} = 38.8$  GeV) and (right) and a function of  $A$  at the SPS (NA50 at  $p_{\text{lab}} = 400$  and 450 GeV) for  $J/\psi$  and  $\psi'$  production.

## PHENIX Has Measured $R_{\text{dAu}}$ for $\psi'$ and $\chi_c$

$R_{\text{dAu}} \sim 0.77 \pm 0.02 \pm 0.16, (0.81 \pm 0.12 \pm 0.23), 0.77 \pm 0.41 \pm 0.18, 0.54 \pm 0.11^{+0.16}_{-0.19}$  for inclusive (direct)  $J/\psi$ ,  $\chi_c$  and  $\psi'$  respectively

$\chi_c$   $A$  dependence never measured in fixed-target experiments, singlet production of  $\chi_c$  could lead to different absorption pattern

Dramatic difference in  $N_{\text{bin}}$  dependence of  $J/\psi$  and  $\psi'$ , not seen previously in  $pA$  but never measured vs. centrality before

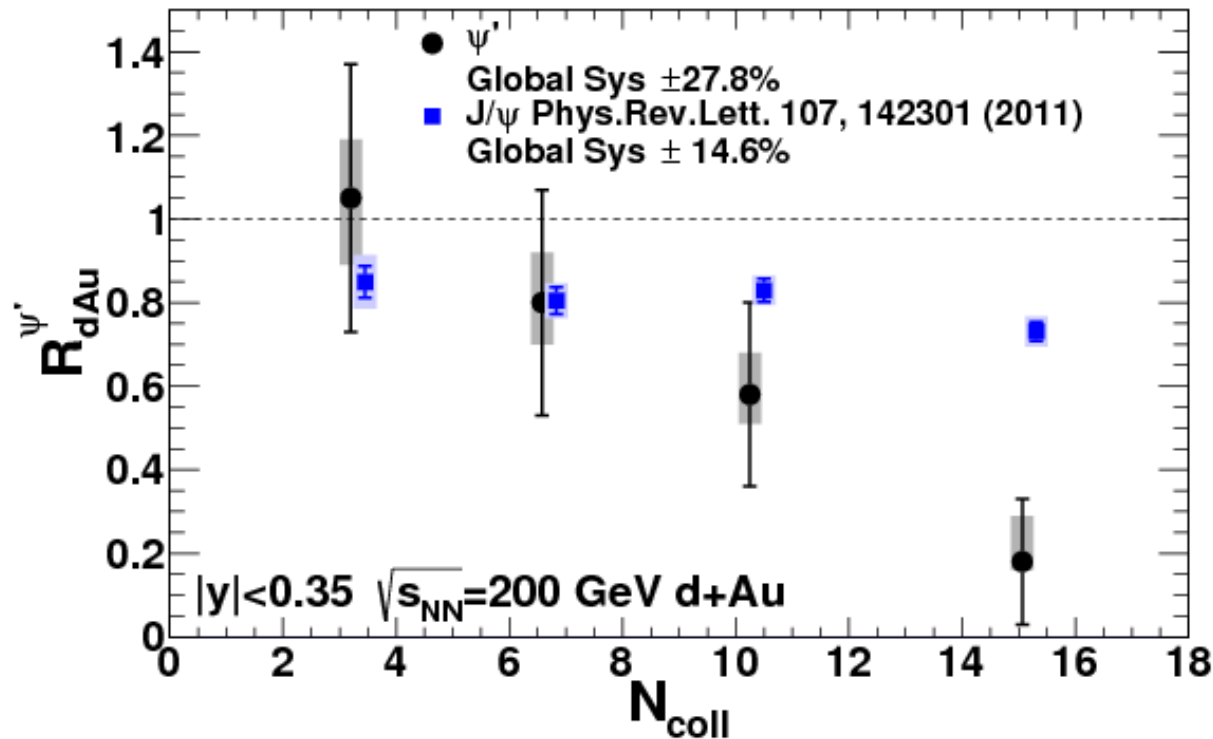


Figure 16: The  $J/\psi$  and  $\psi'$   $N_{\text{coll}}$  dependence as reported by PHENIX. [arXiv:1305.5516]

What's New?

# $R_{p\text{Pb}}$ in $\sqrt{s} = 5 \text{ TeV}$ $p+\text{Pb}$ at the LHC

As expected, NLO shadowing alone does not describe curvature of data

Energy loss with shadowing overestimates effect at forward rapidity

CGC calculations (not shown) fall even further below data

$R_{p\text{Pb}}$  problematic because no measured  $pp$  denominator ( $R_{p\text{Pb}}^{\psi'} < R_{p\text{Pb}}^{J/\psi}$  here also)

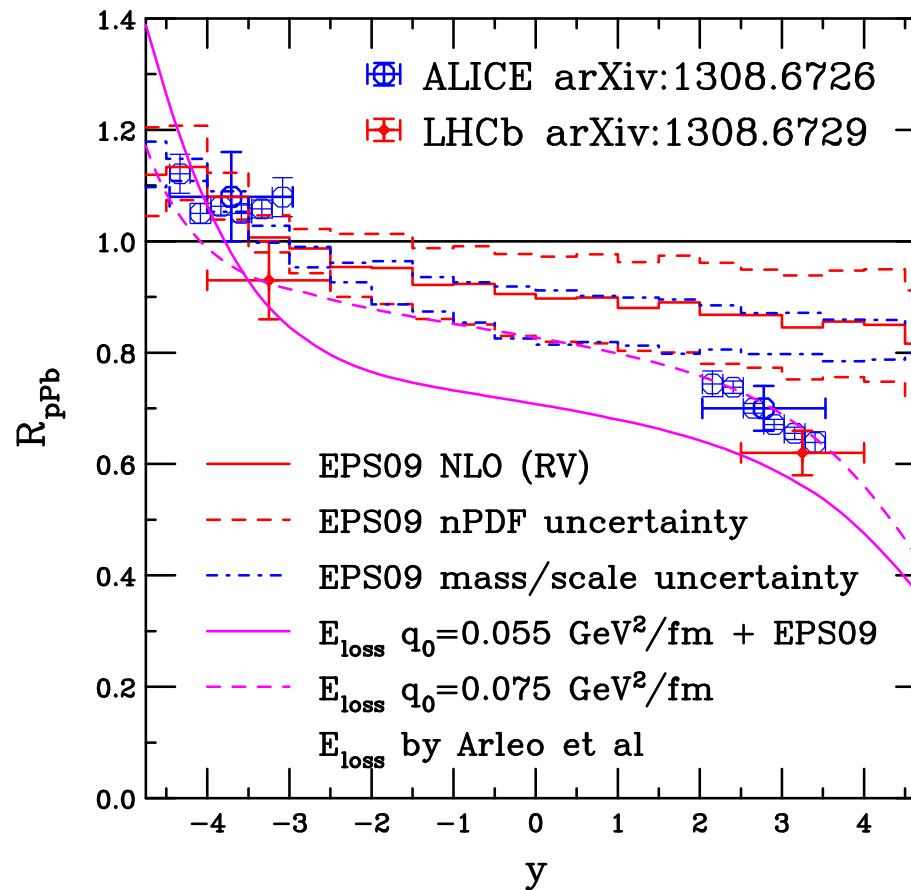


Figure 17: The  $R_{p\text{Pb}}$  ratio for  $J/\psi$  as a function of  $y$ . The dashed red histogram shows the EPS09 uncertainties while the dot-dashed blue histogram shows the dependence on mass and scale. The  $pp$  denominator is also calculated at 5 TeV (which isn't available experimentally). The energy loss calculations of Arleo and Peigne are shown in magenta.

# Calculating Uncertainties in $pA$

The one standard deviation uncertainties on the quark mass and scale parameters calculated using EPS09 central set

If the central, upper and lower limits of  $\mu_{R,F}/m$  are denoted as  $C$ ,  $H$ , and  $L$  respectively, then the seven sets corresponding to the scale uncertainty are

$$(\mu_F/m, \mu_F/m) = (C, C), (H, H), (L, L), (C, L), (L, C), (C, H), (H, C)$$

The extremes of the cross sections with mass and scale are used to calculate the uncertainty

$$\begin{aligned}\sigma_{\max} &= \sigma_{\text{cent}} + \sqrt{(\sigma_{\mu, \max} - \sigma_{\text{cent}})^2 + (\sigma_{m, \max} - \sigma_{\text{cent}})^2} , \\ \sigma_{\min} &= \sigma_{\text{cent}} - \sqrt{(\sigma_{\mu, \min} - \sigma_{\text{cent}})^2 + (\sigma_{m, \min} - \sigma_{\text{cent}})^2} ,\end{aligned}$$

Uncertainties due to shadowing calculated using 30+1 error sets of EPS09 NLO added in quadrature, uncertainty is cumulative

## Final-State Energy Loss (Arleo and Peigne)

Arleo and Peigne fit an energy loss parameter that also depends on  $L_A$  to E866 data and uses the same parameter for other energies

$$\frac{1}{A} \frac{d\sigma_{pA}(x_F)}{dx_F} = \int_0^{E_p-E} d\epsilon P(\epsilon) \frac{d\sigma_{pp}(x_F + \delta x_F(\epsilon))}{dx_F}$$

There is no production model, only a parameterization of the  $pp$  cross section

$$\frac{d\sigma_{pp}}{dp_T dx} = \frac{(1-x)^m}{x} \left( \frac{p_0^2}{(p_0^2 + p_T^2)} \right)^m$$

Parameters  $n$  and  $m$  are fit to  $pp$  data,  $n \sim 5$  at  $\sqrt{s} = 38.8$  GeV, 34 at 2.76 TeV

Including shadowing as well as energy loss modifies the energy loss parameter, no significant difference in shape of fit at fixed-target energy but significant difference at higher  $\sqrt{s}$

Backward  $x_F/y$  effect is large for this scenario

# $R_{F/B}$ Because $p$ +Pb Rapidity Distributions Asymmetric

Forward (+ $y$ ) to backward ( $-y$ ) ratio preferable because no  $pp$  normalization required for data

Data are flatter in  $y$  than the calculations

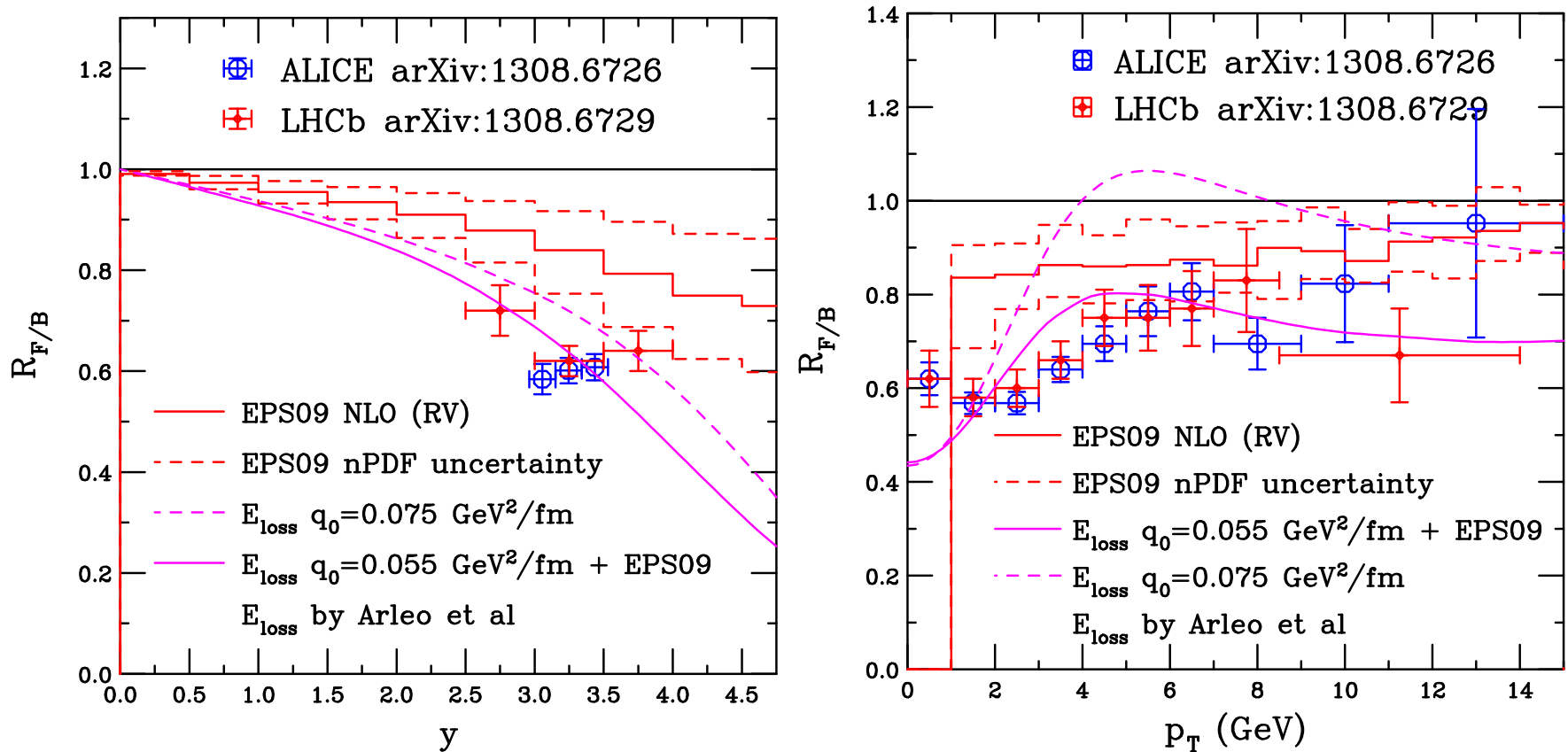


Figure 18: The  $R_{F/B}$  ratios for  $J/\psi$  as a function of  $y$  (left) and  $p_T$  (right). The dashed red histogram shows the EPS09 uncertainties. The energy loss calculations of Arleo and Peigne are shown in magenta.

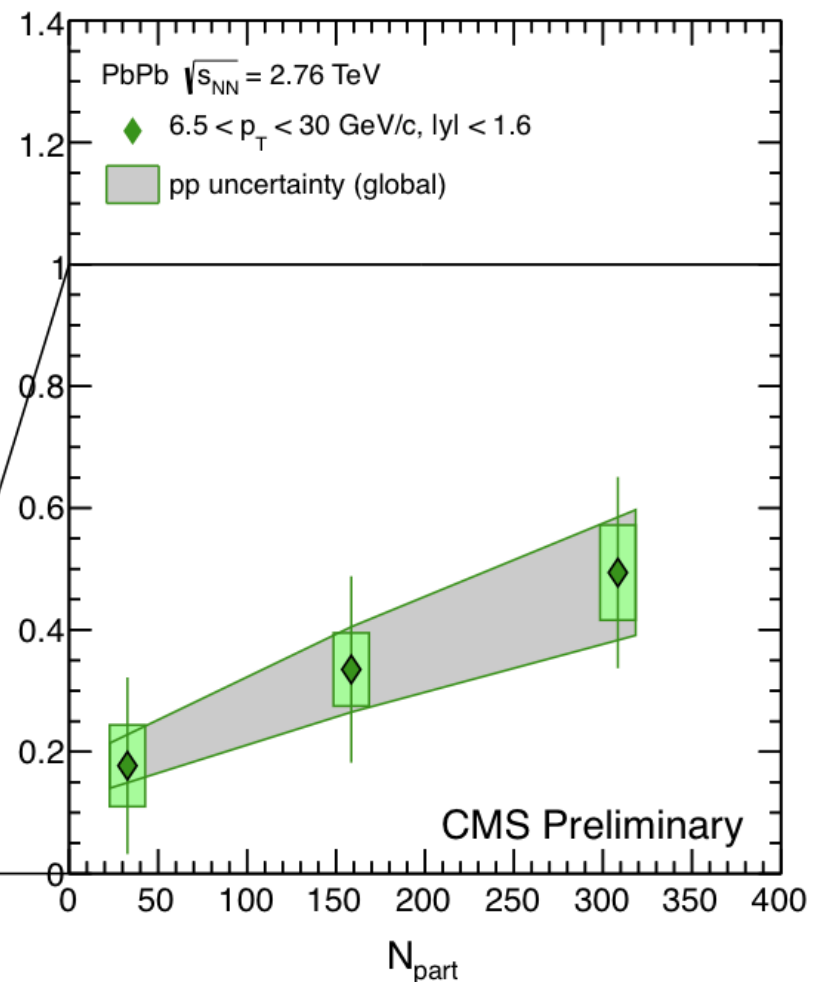
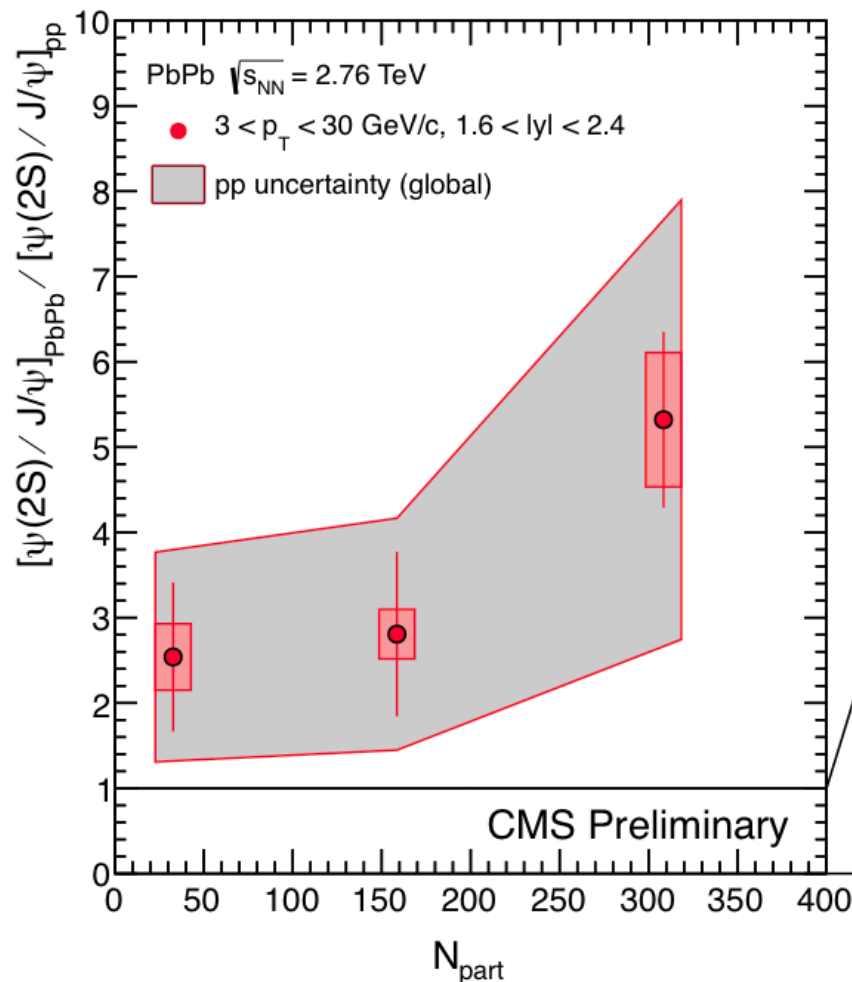
# $\psi'$ Difficult to Interpret in Pb+Pb as Well

CMS forms double ratio of  $\psi'/\psi$  in Pb+Pb relative to  $pp$  collisions

Central collisions,  $|y| < 1.6$ , and high  $p_T$ ,  $p_T > 6.5$  GeV give ratio less than unity

More forward collisions,  $1.6 < |y| < 2.4$ , and lower  $p_T$ ,  $p_T > 3$  GeV gives ratio significantly greater than unity – **Can it all come from coalescence???**

Interpretation depends on  $pp$  baseline but poor statistics, the probable culprit





## Summary .

- Gerry and the Stony Brook Nuclear Theory Group were a big influence in my life and career .
- I've always felt like one of Gerry's kids even if not his officially
- He accepted 2 Physics Reports from me on related subjects, one came out in '99 (I did the proofs while in the hospital having Kristina, they still remember well at Elsevier) and the other in '08 (Me to Gerry: "Don't you even want to know what it's about?") .
- $J/\psi$ 's are still hard ;-)